Supplemental: Hidden prompt splashing by corona splashing at drop impact on a smooth dry surface

Taku Ashida, Masao Watanabe,* Kazumichi Kobayashi, and Hiroyuki Fujii
Division of Mechanical and Space Engineering, Hokkaido University, Sapporo 060-8628, Japan

Toshiyuki Sanada
Department of Mechanical Engineering, Shizuoka University, Hamamatsu, Japan
(Dated: December 25, 2019)

I. SUPPLEMENTARY MOVIES

The supplementary movies of prompt splashing and corona splashing are available. In each movie, the frame number $F_\#$ starting with 0 is indicated on the lower right corner in each image of the movie. The surrounding gas pressure P, impact velocity V, and drop diameter D along with the brief explanations of these movies are listed in Table I.

We showed the occurrence of prompt splashing in Fig. 2. Figures 2(a), (b), and (c) are the selected images from Movie 1, Movie 2, and Movie 3, respectively.

In Movie 1, prompt splashing is observed at $F_\# = 36$, where ejection of jets, presumably fast-moving fine droplets, fly along the solid wall. In this frame, the jet mirror images reflected on the solid surface are also captured. It seems as if the real and mirror images were a pair of parallel lines along the solid surface. They can be observed in the range that $36 \leq F_\# \lesssim 39$. The ejection of jets on the left side of the images are more easily visually recognized. Corona Type-I splashing can be observed at $F_\# = 38$; then, liquid jets, presumably fingers, develops in the obliquely upward.

In Movie 2, prompt splashing is observed at $F_\# = 55$, where fast-moving fine droplets fly along the solid surface in the range that $55 \leq F_\# \lesssim 62$. The liquid film flow develops along the solid surface when $58 \leq F_\#$; then, corona Type-II splashing can be observed.

In Movie 3, prompt splashing is observed at $F_\# = 4$, where fast-moving fine droplets fly along the solid surface in the range that $4 \leq F_\# \lesssim 93$. The smooth liquid film flow is developed in the range that $13 \leq F_\#$.

In Movie 4, prompt splashing is observed at $F_\#59$, where fast-moving fine droplets fly along the solid surface in the range that $59 \leq F_\# \lesssim 66$. The smooth liquid film flow is developed in the range that $62 \leq F_\#$.

In Movie 5, prompt splashing is observed at $F_\# = 13$, where fast-moving fine droplets fly along the solid surface in the range that $13 \leq F_\# \lesssim 86$. The smooth liquid film flow is developed in the range that $19 \leq F_\#$.

In Movie 6, prompt splashing is observed at $F_\# = 28$, where fast-moving fine droplets fly along the solid surface in the range that $28 \leq F_\# \lesssim 50$. The smooth liquid film flow is developed in the range that $33 \leq F_\#$.

TABLE I. Experimental conditions of movies that captured various types of splashing observed immediately after the impact of a water drop on a solid surface.

	P (kPa)	V (m/s)	D (mm)	Remarks
Movie 1	75.1	25.8	2.42	Prompt splashing & corona Type-I splashing
Movie 2	64.5	14.8	2.35	Prompt splashing & corona Type-II splashing
Movie 3	0.8	9.65	2.27	Prompt splashing only
Movie 4	29.5	25.5	2.16	Prompt splashing only
Movie 5	5.7	11.3	2.29	Prompt splashing only
Movie 6	28.8	10.7	2.19	Prompt splashing only
Movie 7	49.8	11.3	2.13	Prompt splashing only
Movie 8	97.9	14.1	2.14	Indistinguishable
Movie 9	100.2	28.4	2.13	Indistinguishable

* masao.watanabe@eng.hokudai.ac.jp

TABLE II. Physical properties and radii of saturated water drops with c_{o_2} of 8.4 mg/L (■, □) and degassed water drops with c_{o_2} of 2.5 ∼ 3.5 mg/L (♦, ◊). The filled and open symbols indicate the cases of occurrence and non-occurrence of prompt splashing, respectively.

		V (m/s)	P (kPa)	σ (mN/m)	ν_ℓ (μm^2/s)	ρ_ℓ (kg/m^3)	D (mm)
(a)	■	10.7	29.9	72.6	0.997	998	2.17
		11.5	28.7	72.3	0.952	998	2.17
		10.7	29.4	72.4	0.971	998	2.20
		10.7	28.8	72.4	0.973	998	2.19
		9.65	29.7	72.5	0.995	998	2.18
		9.38	29.5	72.5	0.981	998	2.20
(b)	□	8.85	30.0	72.5	0.987	998	2.18
		8.85	29.4	72.8	1.04	998	2.18
		9.65	29.7	73.2	1.12	999	2.06
		8.04	29.0	72.5	0.984	998	2.15
		7.50	29.0	72.4	0.963	998	2.20
		6.43	28.6	72.4	0.973	998	2.19
		7.23	28.6	72.4	0.971	998	2.19
(c)	♦	9.65	29.2	72.9	1.07	998	2.23
		9.65	29.5	72.8	1.05	998	2.21
		10.7	29.1	72.8	1.04	998	2.22
		9.65	29.7	72.8	1.04	998	2.24
		8.58	29.3	72.9	1.06	998	2.23
		9.65	29.3	72.8	1.05	998	2.22
(d)	◊	8.58	30.0	72.9	1.06	998	2.21
		7.50	29.1	72.9	1.07	998	2.21
		9.65	28.5	72.9	1.07	998	2.21
		8.58	29.9	72.8	1.05	998	2.22
		8.04	29.9	72.8	1.05	998	2.20

In Movie 7, prompt splashing is observed at $F_\# = 76$, where fast-moving fine droplets fly along the solid surface in the range that $76 \leq F_\#$. The smooth liquid film flow is developed in the range that $85 \leq F_\#$.

In Movies 8 and 9 ($P \gtrsim 90$ kPa), we cannot clearly distinguish prompt splashing from corona splashing with the spatial and temporal resolution in our experiments. However, in Movie 5, it seems that prompt splashing is observed at $F_\# = 68$; then, the liquid film is observed at $F_\# = 70$; later, corona splashing becomes visible at $F_\# = 72$.

II. PHYSICAL PROPERTIES OF LIQUIDS AND EXPERIMENTAL CONDITIONS IN FIGURE 4

The physical properties of various liquids used to produce the experimental results shown in Fig. 4 in the manuscript are listed in Tables II to V. The impact velocity V, surrounding gas pressure P, surface tension σ, liquid kinetic viscosity v_ℓ, liquid density ρ_ℓ, and drop diameter D.

We used saturated water with c_{o_2} of 8.4 mg/L (■, □), and degassed water drops with c_{o_2} of 2.5 ∼ 3.5 mg/L ((♦, ◊)), in order to examine the contribution of the phase change, possibly cavitation, to the occurrence of prompt splashing. The physical properties of these waters [1] and drop diameters are listed in Table II.

We also used alcohol to examine the contributions of liquid physical properties [1–4]: surface tension σ, liquid kinetic viscosity ν_ℓ and liquid density ρ_ℓ, and drop diameter D to the occurrence of prompt splashing. We varied the ethanol drop diameters by using needles with different gauge (22G, 27G, 30G). Physical properties and diameters of ethanol drops released from needle of 22G (▲, △), 27G (▼, ▽), and 30G (►, ▷) are listed in Table III.

We used 1-propanol and 1-butanol to examine the contribution of liquid viscosity to the occurrence of prompt splashing. Physical properties and diameters of 1-propanol drops (■, □) and 1-butanol drops (♦, ◊) are listed in Table IV.

We also used the aqueous solution of 10 %, 20 % and 80 % ethanol. Physical properties and diameters of aqueous solution of 10 % (▲, △), 20 % (▼, ▽), and 80 % (◄, ◁) ethanol drops are listed in Table V. The filled and open symbols indicate the cases of occurrence and non-occurrence of prompt splashing, respectively.

TABLE III. Physical properties and radii of ethanol drops released from needle of 22G (▲, △), 27G (▼, ▽), and 30G (▶, ▷). The filled and open symbols indicate the cases of occurrence and non-occurrence of prompt splashing, respectively.

		V (m/s)	P (kPa)	σ (mN/m)	ν_ℓ (μm^2/s)	ρ_ℓ (kg/m^3)	D (mm)
(e)	▲	10.7	30.2	22.7	1.50	789	2.23
		9.38	29.3	22.8	1.52	789	2.28
		8.58	29.1	22.8	1.52	789	2.25
		9.65	30.5	22.8	1.53	790	2.25
		6.43	30.0	22.8	1.53	790	2.16
		7.23	30.0	22.8	1.53	789	2.27
		6.43	30.0	22.7	1.50	789	2.28
		8.04	29.2	22.6	1.47	788	2.32
		7.77	29.4	22.7	1.49	788	2.23
		6.43	29.6	22.6	1.45	787	2.32
		7.23	29.2	22.7	1.48	788	2.31
		5.89	29.3	22.6	1.46	788	2.34
		5.89	30.7	22.5	1.44	787	2.31
		6.16	28.7	22.7	1.49	788	2.30
(f)	△	6.16	29.8	22.8	1.51	789	2.27
		5.89	30.3	22.7	1.48	788	2.31
		4.28	30.1	22.6	1.46	787	2.30
(g)	▼	9.65	28.4	22.6	1.45	787	1.83
		9.65	28.9	22.6	1.45	787	1.82
		9.65	30.2	22.5	1.44	787	1.83
		11.3	28.8	22.6	1.45	787	1.84
(h)	▽	8.04	29.0	22.6	1.45	787	1.83
		8.58	28.8	22.6	1.45	787	1.84
		9.65	29.2	22.6	1.45	787	1.83
(i)	▶	10.7	30.1	22.9	1.57	791	1.69
		10.7	29.2	23.0	1.58	791	1.68
		10.5	29.7	22.9	1.56	790	1.69
		10.5	29.4	23.0	1.58	791	1.69
(j)	▷	9.65	29.9	22.9	1.55	790	1.68
		8.04	28.7	22.9	1.57	791	1.68
		9.65	29.3	22.9	1.57	791	1.69
		7.23	30.0	22.9	1.57	791	1.69
		8.85	28.8	23.0	1.59	791	1.70
		8.85	29.3	22.9	1.55	790	1.68
		8.58	29.4	23.0	1.59	791	1.69

III. EFFECT OF SURROUNDING GAS ON PROMPT SPLASHING

We found that the pressure of the surrounding gas is irrelevant to determining whether prompt splashing occurs, while the impact velocity V is essential. We examine the threshold velocity for prompt splashing $V_{\rm pr}$ in various species of gases in order to investigate whether the occurrence of prompt splashing is independent of the surrounding gas. Fig. 1 shows the occurrence of prompt splashing in air, helium, and carbon dioxide.

The gas speed of sound a_g and gas viscosity μ_g are the physical properties independent of gas pressure. In order to examine the role of these properties on the occurrence of prompt splashing, we used helium, whose a_g is approximately thrice as large as a_g of air, and carbon dioxide, whose μ_g is approximately four-fifths of μ_g of air. The physical properties of air, helium and carbon dioxide are listed in Table VI.

We evaluated $V_{\rm pr}$'s in air, helium, and carbon dioxide, and the results do not show any significant differences. Considering this result, there is sufficient evidence to conclude that $V_{\rm pr}$ is independent of the surrounding gas.

It is well known that a liquid drop impacting a stationary solid surface deforms before the liquid drop makes contact with the stationary solid surface [5, 6], or it entraps a small air disk under its center [7–9]. The formation of the central air disk is characterized by the Stokes number ${\rm St} = \mu_g/(\rho_\ell RV)$, the compressibility factor $\epsilon = P/(RV^7\rho_\ell^4/\mu_g)^{1/3}$, and the Knudsen number ${\rm Kn} = \lambda/(R{\rm St}^{2/3})$ [9–12]. Li *et al.* [9] experimentally investigated the effects of reduced pressure on the air-disc dynamics under an impacting drop on a stationary solid surface in a similar range of St values as those found in our experiments and with impact velocities reaching 5.1 m/s.

TABLE IV. Physical properties and radii of 1-propanol drops (■, □) and 1-butanol drops (♦, ◊). The filled and open symbols indicate the cases of occurrence and non-occurrence of prompt splashing, respectively.

		V (m/s)	P (kPa)	σ (mN/m)	ν_ℓ (μm^2/s)	ρ_ℓ (kg/m^3)	D (mm)
(k)	■	8.85	28.6	23.7	2.49	800	2.20
		8.85	29.2	23.7	2.49	800	2.35
		8.58	29.8	23.7	2.49	800	2.37
		7.77	29.2	23.7	2.49	800	2.23
		7.77	29.7	23.7	2.49	800	2.34
		8.85	29.4	23.7	2.49	800	2.32
		9.65	29.4	23.7	2.49	800	2.30
(l)	□	7.23	29.7	23.7	2.49	800	2.33
		7.77	29.9	23.7	2.49	800	2.35
		7.23	28.9	23.7	2.49	800	2.33
		6.96	29.3	23.7	2.49	800	2.34
(m)	♦	10.7	29.7	24.6	3.23	806	2.31
		11.3	28.7	24.6	3.23	806	2.30
		9.65	29.0	24.6	3.23	806	2.31
		10.2	29.5	24.6	3.23	806	2.30
		10.7	30.5	24.6	3.23	806	2.32
		11.3	29.6	24.6	3.23	806	2.35
(n)	◊	10.7	28.9	24.6	3.23	806	2.31
		8.04	29.8	24.6	3.23	806	2.31
		10.7	29.8	24.6	3.23	806	2.28
		7.23	29.9	24.6	3.23	806	2.31
		8.85	29.4	24.6	3.23	806	2.30
		9.65	29.7	24.6	3.23	806	2.32
		9.65	30.1	24.6	3.23	806	2.30

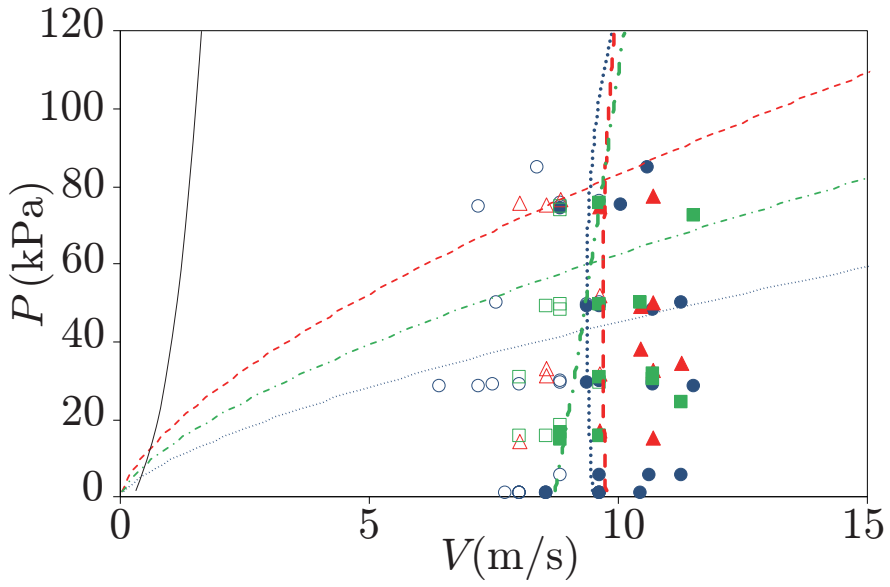

FIG. 1. Prompt splashing at P =1, 5, 15, 30, 50, and 75 kPa in air (●,○), He (▲,△) and CO_2 (■, □) with respect to V and P. The filled and open symbols indicate whether prompt splashing is observed or not, respectively. The criteria are shown by the blue dotted (· · ·), red dashed (- - -), and green dot-dash (- · -) lines for air, He, and CO_2, respectively. The Stokes number at V=10 m/s in air is 1.70 × 10^{-6}. The condition where ϵ=1 is shown with a black line and where Kn=1 are shown with thin dotted (· · ·), thin dashed (- - -), and thin dot-dash (- · -) lines for air, He, and CO_2, respectively.

TABLE V. Physical properties and radii of aqueous solution of 10 % (▲, △), 20 % (▼, ▽), and 80 % (◀, ◁) ethanol drops. The filled and open symbols indicate the cases of occurrence and non-occurrence of prompt splashing, respectively.

		V (m/s)	P (kPa)	σ (mN/m)	ν_ℓ (μm^2/s)	ρ_ℓ (kg/m^3)	D (mm)
(o)	▲	8.58	29.2	48.9	1.29	980	2.45
		7.77	29.4	48.9	1.29	980	2.48
		8.04	29.3	48.9	1.29	980	2.45
		7.77	30.1	48.9	1.29	980	2.48
(p)	△	7.50	30.5	48.9	1.29	980	2.47
		7.23	29.3	48.9	1.29	980	2.38
(q)	▼	8.85	28.3	39.8	1.84	965	2.31
		9.65	29.0	39.8	1.84	965	2.31
(r)	▽	8.04	29.2	39.8	1.84	965	2.32
		7.77	29.5	39.8	1.84	965	2.29
		8.85	29.2	39.8	1.84	965	2.29
		8.85	30.2	39.8	1.84	965	2.38
		8.58	29.1	39.8	1.84	965	2.31
		8.04	28.7	39.8	1.84	965	2.30
(s)	◀	9.65	29.3	25.5	2.26	845	2.33
		9.65	29.6	25.5	2.26	845	2.31
		8.58	29.9	25.5	2.26	845	2.31
(t)	◁	7.23	28.6	25.5	2.26	845	2.30
		8.04	30.2	25.5	2.26	845	2.30
		7.77	28.2	25.5	2.26	845	2.34
		8.04	29.8	25.5	2.26	845	2.32
		8.85	29.9	25.5	2.26	845	2.34
		9.65	30.3	25.5	2.26	845	2.33

TABLE VI. Physical properties of the different gas used ($P = 10^5$ Pa and $T = 298.15$ K).

	ρ_g (kg/m^3)	μ_g (μPa·s)	a_g (m/s)
Air	1.1609	18.62	347.4
He	0.1604	19.93	1019.6
CO_2	1.773	14.91	269.4

It was found that the air-disk dynamics drastically change for $\mathrm{Kn} \geq 1$, indicating that the gas is significantly rarefied. If air were entrapped in our impact conditions, the transition to the rarefied gas regime could cause the air-disk dynamics to change. Thus, whether prompt splashing occurs should be dependent on Kn. However, the threshold velocities V_{pr}'s are independent of Kn, as shown in Fig. 1.

Furthermore, predicting an initial air-disk radius $L_0 \sim \epsilon^{0.15}\mathrm{Kn}^{-0.57}\mathrm{St}^{1/3}R$ in adiabatic conditions ($\gamma_g = 1.4$) [9] if air were entrapped indicates by a factor of at least 20 in the air-disk radii ($L_0 \sim 1.3 \times 10^{-4}$ m for $P = 80$ kPa and $5.6{\times}10^{-6}$ m for $P = 1$ kPa) in our impact conditions. However, V_{pr} is independent of the gas pressure, as shown in Fig. 1.

Considering these results, the sir-disk dynamics may not affect the occurrence of prompt splashing. This result is a counterevidence to the previous experimental observations [13] that reducing the ambient-gas pressure inhibits prompt splashing in low Oh liquid (i.e., ethanol). Our experimental results indicate that reducing ambient-gas pressure may increase both sizes and numbers of droplets because prompt splashing in Movie 5 can be observed more clearly than that in Movie 3, although reducing the ambient-gas pressure does not alter the threshold velocity V_{pr}.

[1] H. Uchida, *JSME Data Book : The Thermophysical Properties of Fluids* (The Japan Society of Mechanical Engineers, Tokyo, 1983) Chap. 2.

[2] I. S. Khattab, F. Bandakarr, r. A. A. F. Author, and A. Jouyban, Density, viscosity, and surface tension of water+ethanol mixtures from 293 to 323K, Korean Journal of Chemical Engineering **29**, 812 (2012).

[3] H. S. Ashbaugh, J. Wesley Barnett, A. Saltzman, M. E. Langrehr, and H. Houser, Communication: Stiffening of dilute alcohol and alkane mixtures with water, Journal of Chemical Physics **145**, 201102 (2016).
[4] N. V. Sastry and M. K. Valand, Densities, speeds of sound, viscosities, and relative permittivities for 1-propanol + and 1-butanol + heptane at 298.15 K and 308.15 K, Journal of Chemical and Engineering Data **41**, 1421 (1996).
[5] R. C. A. van der Veen, T. Tran, D. Lohse, and C. Sun, Direct measurements of air layer profiles under impacting droplets using high-speed color interferometry, Physical Review E **85**, 1 (2012).
[6] P. D. Hicks and R. Purvis, Air cushioning in droplet impacts with liquid layers and other droplets, Physics of Fluids **23**, 10.1063/1.3602505 (2011).
[7] E. Q. Li, I. U. Vakarelski, and S. T. Thoroddsen, Probing the nanoscale: the first contact of an impacting drop, Journal of Fluid Mechanics **785**, R2 (2015).
[8] C. Josserand and S. T. Thoroddsen, Drop Impact on a Solid Surface, Annual Review of Fluid Mechanics **48**, 365 (2016).
[9] E. Q. Li, K. R. Langley, Y. S. Tian, P. D. Hicks, and S. T. Thoroddsen, Double Contact during Drop Impact on a Solid under Reduced Air Pressure, Physical Review Letters **119**, 214502 (2017).
[10] S. Mandre, M. Mani, and M. P. Brenner, Precursors to Splashing of Liquid Droplets on a Solid Surface, Physical Review Letters **102**, 4 (2009).
[11] S. Mandre and M. P. Brenner, The mechanism of a splash on a dry solid surface, Journal of Fluid Mechanics **690**, 148 (2012).
[12] L. Duchemin and C. Josserand, Rarefied gas correction for the bubble entrapment singularity in drop impacts, Comptes Rendus - Mecanique **340**, 797 (2012), arXiv:1208.0159.
[13] A. Latka, A. Strandburg-Peshkin, M. M. Driscoll, C. S. Stevens, and S. R. Nagel, Creation of Prompt and Thin-Sheet Splashing by Varying Surface Roughness or Increasing Air Pressure, Physical Review Letters **109**, 054501 (2012).